

High-Linear Energy Transfer (LET) α versus Low-LET β Emitters in Radioimmunotherapy of Solid Tumors: Therapeutic Efficacy and Dose-limiting Toxicity of ^{213}Bi - versus ^{90}Y -labeled CO17-1A Fab' Fragments in a Human Colonic Cancer Model¹

Thomas M. Behr,² Martin Béhé, Michael G. Stabin, Eike Wehrmann, Christos Apostolidis, Roger Molinet, Frank Strutz, Afshin Fayyazi, Eberhard Wieland, Stefan Gratz, Lothar Koch, David M. Goldenberg, and Wolfgang Becker

Departments of Nuclear Medicine [T. M. B., M. B., E. We., S. G., W. B.], Internal Medicine (Nephrology) [F. S.], Pathology [A. F.], and Clinical Chemistry [E. Wi.], Georg-August-University, Göttingen D-37075, Germany; Oak Ridge Institute for Science and Education, Oak Ridge, Tennessee 37831 [M. G. S.]; Institute for Transuranium Elements, D-76125 Karlsruhe, Germany [C. A., R. M., L. K.]; and Garden State Cancer Center, Belleville, New Jersey 07109 [D. M. G.]

ABSTRACT

Recent studies suggest that radioimmunotherapy (RIT) with high-linear energy transfer (LET) radiation may have therapeutic advantages over conventional low-LET (e.g., β^-) emissions. Furthermore, fragments may be more effective in controlling tumor growth than complete IgG. However, to the best of our knowledge, no investigators have attempted a direct comparison of the therapeutic efficacy and toxicity of a systemic targeted therapeutic strategy, using high-LET α versus low-LET β emitters *in vivo*. The aim of this study was, therefore, to assess the toxicity and antitumor efficacy of RIT with the α emitter $^{213}\text{Bi}/^{213}\text{Po}$, as compared to the β emitter ^{90}Y , linked to a monovalent Fab' fragment in a human colonic cancer xenograft model in nude mice.

Biodistribution studies of ^{213}Bi - or ^{88}Y -labeled benzyl-diethylene-triamine-pentaacetate-conjugated Fab' fragments of the murine monoclonal antibody CO17-1A were performed in nude mice bearing s.c. human colon cancer xenografts. ^{213}Bi was readily obtained from an "in-house" $^{225}\text{Ac}/^{213}\text{Bi}$ generator. It decays by β^- and 440-keV γ emission, with a $t_{1/2}$ of 45.6 min, as compared to the ultra-short-lived α emitter, ^{213}Po ($t_{1/2} = 4.2 \mu\text{s}$). For therapy, the mice were injected either with ^{213}Bi - or ^{90}Y -labeled CO17-1A Fab', whereas control groups were left untreated or were given a radiolabeled irrelevant control antibody. The maximum tolerated dose (MTD) of each agent was determined. The mice were treated with or without inhibition of the renal accretion of antibody fragments by D-lysine (T. M. Behr *et al.*, *Cancer Res.*, 55: 3825–3834, 1995), bone marrow transplantation, or combinations thereof. Myelotoxicity and potential second-organ toxicities, as well as tumor growth, were monitored at weekly intervals. Additionally, the therapeutic efficacy of both ^{213}Bi - and ^{90}Y -labeled CO17-1A Fab' was compared in a GW-39 model metastatic to the liver of nude mice.

In accordance with kidney uptake values of as high as $\geq 80\%$ of the injected dose per gram, the kidney was the first dose-limiting organ using both ^{90}Y - and ^{213}Bi -labeled Fab' fragments. Application of D-lysine decreased the renal dose by >3 -fold. Accordingly, myelotoxicity became dose limiting with both conjugates. By using lysine protection, the MTD of ^{90}Y -Fab' was 250 μCi and the MTD of ^{213}Bi -Fab' was 700 μCi , corresponding to blood doses of 5–8 Gy. Additional bone marrow transplantation allowed for an increase of the MTD of ^{90}Y -Fab' to 400 μCi and for ^{213}Bi -Fab' to 1100 μCi , respectively. At these very dose levels, no biochemical or histological evidence of renal damage was observed (kidney doses of <35 Gy). At equitoxic dosing, ^{213}Bi -labeled Fab' fragments were significantly more effective than the respective ^{90}Y -labeled conjugates. In the metastatic model, all untreated controls died from rapidly progressing hepatic metastases at 6–8 weeks after

tumor inoculation, whereas a histologically confirmed cure was observed in 95% of those animals treated with 700 μCi of ^{213}Bi -Fab' 10 days after model induction, which is in contrast to an only 20% cure rate in mice treated with 250 μCi of ^{90}Y -Fab'.

These data show that RIT with α emitters may be therapeutically more effective than conventional β emitters. Surprisingly, maximum tolerated blood doses were, at 5–8 Gy, very similar between high-LET α and low-LET β emitters. Due to its short physical half-life, ^{213}Bi appears to be especially suitable for use in conjunction with fast-clearing fragments.

INTRODUCTION

RIT³ is an attractive therapeutic concept, aiming to deliver tumoricidal radiation doses to tumors without causing significant radiation toxicity to normal tissues (1). Indeed, in radiosensitive tumors, such as non-Hodgkin's lymphoma, RIT has led to long-term remissions and even cures in a high percentage of treated patients (1–3). In solid tumors, however, success is still limited, probably due to the relatively low specific accretion of the radiolabeled antibody in the tumor target as compared to the normal tissues (1, 4, 5).

More recently, the use of high-LET radiation emitters has been proposed (6–9). One such approach is the use of Auger/conversion electron emitters, which requires their conjugation to carriers (e.g., antibodies) that internalize selectively into the target cancer cells. Due to their short path length, these low-energy Auger electrons can reach the nuclear DNA only if the antibody is internalized, such as in antigen-expressing tumor tissue but not in the other nonmalignant cells, e.g., the hematopoietic cells in the red marrow. Indeed, higher antitumor efficacy at lower toxicity has been demonstrated *in vitro* (6) as well as preclinically (7) and clinically (8, 9).

α emitters appear to be an even more attractive therapeutic alternative because, due to their path length of several cell diameters, their high LET radiation does not necessarily require internalization into the target cell (10, 11). Therefore, non-antigen-expressing tumor cells in their neighborhood may also become inactivated. Several α emitters have been proposed for this purpose (reviewed in Ref. 11). Although attractive due its short half-life (7.2 h) and the anticipated similarity of its chemical behavior to the well-understood chemistry of iodine, the halogen ^{211}At is burdened by the long half-life (38 years) of its β -emitting decay product, ^{207}Bi . Furthermore, directly astatinylated tyrosyl moieties have been shown to be metabolically unstable (10); the use of astatinylated *N*-succinimidyl benzoate derivatives yields more stable conjugates but requires a more sophisticated chemical synthesis (10, 12, 13). Radium isotopes (mainly ^{223}Ra , but also ^{224}Ra) have been proposed (1, 11), but no chelator has demonstrated

Received 11/16/98; accepted 4/5/99.

The costs of publication of this article were defrayed in part by the payment of page charges. This article must therefore be hereby marked *advertisement* in accordance with 18 U.S.C. Section 1734 solely to indicate this fact.

¹ Supported in part by Grant Be 1689/4-1 from the Deutsche Forschungsgemeinschaft (to T. M. B.) and Outstanding Investigator Grant CA39841 from the National Cancer Institute (to D. M. G.).

² To whom requests for reprints should be addressed, at Department of Nuclear Medicine, Georg-August-University of Göttingen, Robert-Koch-Strasse 40, D-37075 Göttingen, Germany. Phone: 49-551-39-8510; Fax: 49-551-39-8526; E-mail: tmbehr@med.uni-goettingen.de.

³ The abbreviations used are: RIT, radioimmunotherapy; LET, linear energy transfer; DTPA, diethylene-triamine-pentaacetate; Bz-DTPA, benzyl-DTPA; MTD, maximum tolerated dose; BMT, bone marrow transplantation; BUN, blood urea nitrogen; ID, injected dose; MAb, monoclonal antibody; RBE, relative biological effectiveness.

sufficient stability *in vivo* thus far. ^{212}Bi and its parent ^{212}Pb have been chelated successfully to antibodies and other proteins via DTPA or tetraazacyclododecane- N,N',N'',N''' -tetraacetate derivatives (14, 15); both have already been used for α -RIT, but the decay product of ^{212}Bi , ^{208}Tl is itself a high-energy β^- and γ emitter, potentially raising radiation protection problems. Some years ago, ^{213}Bi was proposed for α immunotherapy (16, 17). It can be readily obtained from an "in-house" $^{225}\text{Ac}/^{213}\text{Bi}$ generator (16, 17). ^{213}Bi decays mainly (98%) by β^- and 440-keV γ emission with a $t_{1/2}$ of 45.6 min to the ultra-short-lived high-energy (8.375-MeV) α emitter ^{213}Po ($t_{1/2} = 4.2 \mu\text{s}$), whereas a direct α decay pathway to ^{209}Tl plays only a negligible role (2% of all ^{213}Bi decays).

Several studies have been published on the therapeutic use of α emitters, and several authors suggested their therapeutic superiority (most recently reviewed in Ref. 11). However, with exception of the study of Bloomer *et al.* (18) using colloids for therapy of malignant ovarian ascites in mice, to the best of our knowledge, no investigators have attempted a direct comparison of the therapeutic efficacy and toxicity of targeted therapy with high-LET α versus low-LET β emitters *in vivo*. Our previous work has shown that (a) monovalent antibody fragments (*e.g.*, Fab') may have therapeutic advantages over bivalent immunoconjugates [*e.g.*, F(ab')₂ or IgG], which is due to a more homogenous intratumoral distribution and higher intratumoral dose rates (19); (b) potential nephrotoxicity of antibody fragments can be overcome successfully (20, 21); and (c) matching biological half-lives of the carrier and physical half-lives of the radionuclides may optimize their therapeutic efficacy (21). Therefore, we chose, for this study, the monovalent Fab' fragment of the MAAb CO17-1A, to assess the toxicity and antitumor efficacy of RIT with the α emitter $^{213}\text{Bi}/^{213}\text{Po}$ as compared to the β emitter ^{90}Y , linked to a monovalent Fab' fragment in a human colon cancer model in nude mice and to correlate the observed biological effects to the calculated radiation dosimetry.

MATERIALS AND METHODS

Antibodies, Radioconjugate Synthesis, and Quality Control. The murine MAAb CO17-1A was obtained from GlaxoWellcome (Hamburg, Germany), as described previously (7, 22–24). It is an IgG2a isotype directed against a M_r 41,000 glycoprotein that is found on human gastrointestinal malignancies and, to a lower extent, on normal epithelia (22–24). It has an affinity constant of 5×10^7 liter/mol to its antigen (7, 22–24). After antigen binding, it is readily internalized into the antigen-expressing tumor cells (6, 7). The antihuman-CD3 antibody, OKT3, was used as irrelevant isotype-matched control (7). OKT3, which is a murine IgG2a as well, was obtained from CILAG (Sulzbach/Taunus, Germany).

Fab' fragments were prepared from complete IgG by pepsin digestion [ImmunoPure F(ab')₂ preparation kit; Pierce, Rockford, IL] and subsequent disulfide reduction in the presence of 10 mM cysteine for 12 h at 37°C. Fab' fragments were purified by protein A chromatography. Isothiocyanate-Bz-DTPA conjugates of iodoacetamide-blocked Fab' fragments were prepared as described previously (21, 25).

Radiolabeling. For biodistribution studies, ^{88}Y was obtained as $^{88}\text{YCl}_3$ in 0.1 M HCl from Amersham Life Science (Braunschweig, Germany). For therapy, ^{90}Y was obtained from Pacific Northwest National Laboratory (Richland, WA) as $^{90}\text{YCl}_3$ in 0.05 M HCl.

^{213}Bi was obtained as mixed iodide/chloride salt (mainly in the form of the BiI_5^{2-} anion; Refs. 11 and 26) from an in-house $^{225}\text{Ac}/^{213}\text{Bi}$ generator, as has been described in more detail previously (16, 17). Briefly, ^{225}Ac , which had been purified from a ^{229}Th source (the latter being a decay product of ^{233}U , originally obtained from the Oak Ridge National Laboratory, Oak Ridge, TN; Refs. 16, 17, 27, and 28) was dissolved in 2 M HCl and loaded onto a lead-shielded 4×40 mm column of AG MP-50 cation exchange resin (Bio-Rad Laboratories, Munich, Germany). ^{225}Ac decays by α/γ decay with a 10.0-day half-life via two short-lived α/γ -emitting intermediates (^{221}Fr and ^{217}At) to ^{213}Bi , which can be eluted in 2-h intervals with 1 ml of 0.1 M NaI-0.1 M HCl. After each elution, the cation exchange column was reequilibrated by

washing with five bed volumes of 0.01 M HCl. The 0.1 M NaI-0.1 M HCl eluate containing the activity was buffered with 200 μl of 0.5 M NaOAc (pH 5.5), and the pH was adjusted with 50–70 μl of 1.0 M NaOH to 5.5.

Radiolabeling of the immunoconjugates followed procedures described previously (21). Briefly, the antibody chelate was buffered in 0.5 M NaOAc (pH 5.5). Activity was added to yield a specific activity of 4–5 mCi/mg antibody protein, and the reaction mixture was incubated for 5 min at 37°C. The labeled chelate was purified from unbound radiolabel within 5 min by size-exclusion chromatography on a PD-10 column (Sephadex G-25 prepacked in a 15×50 mm column; Pharmacia, Uppsala, Sweden). Excess of DTPA was added to each preparation to chelate any unbound bismuth or yttrium, to assure its rapid renal excretion and to prevent eventual kidney or bone accretion. The quality of each preparation was tested by high-performance liquid chromatography (Bio-Sil SEC-250 column, 300×7.8 mm; Bio-Rad Laboratories, Richmond, CA) as well as by measuring its immunoreactivity (21). The amount of unbound isotope was <2%, and 80–85% of the radiolabeled antibodies bound to the GW-39 cells in each preparation. Labeled antibodies were administered within 20 min of their final preparation.

Animal Models (s.c. and Metastatic). Female nude mice, weighing 19–23 g and 4–5 weeks old, were purchased from Charles River (Sulzfeld, Germany). The human colon carcinoma cell line, GW-39 (29), was serially propagated by preparing a mince through a 40-mesh screen and rinsing with sterile HBSS (ICN Biomedicals, Eschwege, Germany) to yield a 20% cell suspension. Two hundred μl of this suspension were injected s.c. After ~10 days, tumors reached the size of ~100–200 mg, which was the size used in this study.

As will be published elsewhere in more detail,⁴ multiple liver metastases of the same human colon cancer cell line, GW-39, were induced by intrasplenic injection of 100 μl of a 10% tumor cell suspension into the spleen of anesthetized nude mice with subsequent splenectomy 2 min later. All animals treated in this manner develop multiple (>250) microscopic tumor colonies in their livers, reaching a size of ~250–500 μm at 10 days and a size of 1–2.5 mm at 20 days after tumor cell inoculation (see Fig. 4C).⁴ With high reproducibility, the animals begin to lose weight by 4–6 weeks and eventually die at 6–9 weeks after tumor inoculation.⁴

Biodistribution Studies. s.c. tumor-bearing animals were injected into the tail vein with the radiolabeled antibody fragments at a protein amount of ~100–200 μg . The mice were sacrificed at 10 min, 1 h, 4 h, 24 h, 72 h, and 168 h for ^{88}Y - and at 10 min, 1 h, 3 h, and 5 h for ^{213}Bi -labeled conjugates. They were bled by retroorbital puncture. For determining the whole-body retention, the mice were measured in a well counter. After cervical dislocation, the animals were dissected. The amount of activity in the tumors and tissues (liver, spleen, kidney, lung, heart, intestine, bone, and blood) was determined by gamma scintillation counting using an injection standard to account for physical decay, as described previously (*e.g.*, Ref. 21). The number of animals used for each study was typically five per group at each time point, and the tumor sizes were in the same range as those used for the actual therapy experiments.

Radiation Dosimetry. The biodistribution data were used to generate time-activity curves (7, 19). Time-activity curves were fit to the difference or sum of two exponents for curves with and without an uptake component, respectively. Cumulated activity in each organ was obtained by analytically integrating the resulting expressions over time.

Tumor and organ doses were calculated, accounting for the electrons of ^{90}Y or the α particle, electron, and photon contributions of ^{213}Bi and its daughter, ^{213}Po , but neglecting the ^{209}Pb or ^{209}Tl β contributions. These dose calculations were performed according to the geometric model of a 30-g mouse by Yoriyaz and Stabin (30). This model accounts for cross-organ irradiation and the whole-body contribution by using the Monte Carlo transport simulation code MCNP4A (30, 31). In this model, typically, ~500,000 particle histories were followed and absorbed fractions and S values were generated for sources in all major organs and the "remainder of the body." Total absorbed doses were also calculated for all important target organs, considering all sources of radiation dose (32). The fractional contribution from cross-irradiation of dif-

⁴ T. M. Behr, A. L. Salib, T. Liersch, M. Béhé, C. Angerstein, R. D. Blumenthal, A. Fayyazi, R. M. Sharkey, B. Ringe, H. Becker, B. Wörmann, W. Hiddemann, D. M. Goldenberg, and W. Becker, W. Radioimmunotherapy of small volume disease of colorectal cancer metastatic to the liver: preclinical evaluation in comparison to standard chemotherapy and initial results of a Phase I clinical study. Clin. Cancer Res., in press, 1999.

ferent organs by electrons was calculated. Normally, this contribution is neglected in internal dose calculations; however, we have shown previously that, in a small animal, it may be significant (7, 21, 32).

Experimental RIT. Tumor sizes of s.c. tumors were determined by caliper measurement in three dimensions immediately before therapy and at weekly intervals thereafter. Animals were either left untreated (controls) or injected with a single dose of ^{90}Y - or ^{213}Bi -labeled CO-1A Fab' with the activities indicated. Ten to 20 animals were studied in each treatment group. As a nonspecific therapy control, the Bz-DTPA-conjugated Fab' fragment of the anti-CD3 human T-cell lymphoma MAb OKT3 was used. Body weight was recorded weekly, and survival was monitored. The MTD was defined as the highest possible dose under the respective conditions that did not result in any animal deaths, with the next higher dose level resulting in at least 10% of the animals dying (21). Animals were observed until their death or a loss of >30% of their original weight or until the tumor began to ulcerate through the skin, at which time they were removed from the group and sacrificed (21).

Renal Uptake Reduction and BMT. D-Lysine monohydrochloride (Sigma Chemie, Deisenhofen, Germany) was dissolved in PBS at 175 mg/ml. The animals were injected i.p. with 200 μl of this solution (i.e., 35 mg of D-lysine) with four hourly injections, starting 30 min before administration of the radiolabeled antibody, as was established previously as the optimal regimen (20, 21).

Bone marrow was harvested by sterile technique from untreated donor nude mice of the same strain. The marrow cavity of both mouse femurs was rinsed with 0.9% sterile saline using 26-gauge needles, as described previously (33). An inoculum of 10^7 bone marrow cells was injected i.v. via the tail vein at 24 h after radioantibody injection.

Determination of Blood Counts and Renal and Liver Function Parameters. Total and differential leukocyte and thrombocyte counts were determined on the day of therapy and at weekly intervals thereafter. Seventy-five- μl heparinized specimens were collected by retroorbital bleeding. The sample were counted on a Technicon H3 Auto-Analyzer (Bayer-Diagnostik, Munich, Germany). The mean \pm SD was calculated for each group. BUN and creatinine as well as glutamate oxaloacetate transaminase and alkaline phosphatase levels were determined on the day of RIT and at weekly intervals thereafter. All these parameters were assayed as described previously (7, 19, 21).

Histology. For organ and tumor histology, the animals were sacrificed by cervical dislocation and necropsied at the times indicated. Organs were fixed in 10% formalin, embedded in paraffin, and cut into 5- μm sections, as described previously (7, 19, 21). Staining was performed with H&E or periodic acid-Schiff.

Statistical Analysis. Differences in the tissue uptake values and the bio-distribution data were statistically analyzed with the Student's *t* test for unpaired data, as described previously (34). Pairwise comparisons were performed with the Wilcoxon rank-sum test (35). Differences in the therapeutic efficacy between the treatment modalities in s.c. tumors were analyzed by assuming an exponential tumor growth pattern; nonlinear regression analysis based on asymptotic approximation was used as described previously (34). Survival analysis was based on the Kaplan-Meier product limit, and groups were compared using the log-rank test. The log-rank test was also used for comparing times to tumor volume multiplication (36, 37).

RESULTS

Biodistribution of Bismuth- versus Yttrium-labeled CO17-1A Fab'. Fig. 1 shows the biodistribution of bismuth- versus yttrium-labeled CO17-1A Fab' (Fig. 1a) as compared to free, unchelated Bi^{3+} or Y^{3+} (Fig. 1b) in tumor, blood, kidneys and bone of s.c. GW-39 tumor-bearing nude mice. Due to the short physical half-life of ^{213}Bi , biodistribution studies were performed up to 5 h postinjection (i.e., more than six physical half-lives), in contrast to 1 week with yttrium-labeled conjugates. No significant differences were observed between the biokinetics of both ^{213}Bi - or ^{88}Y -labeled immunoconjugates. The blood clearance was biexponential, with similar half-lives ($t_{1/2\alpha} \sim 15$ min, $t_{1/2\beta} \sim 5$ h) to those observed with radioiodinated Fab' fragments (19). The uptake in the tumor was rapid, reaching its apogee as early as after 1–4 h postinjection ($\sim 4\%$ ID/g). As expected with monovalent Fab', renal accretion was predominant, with maximum

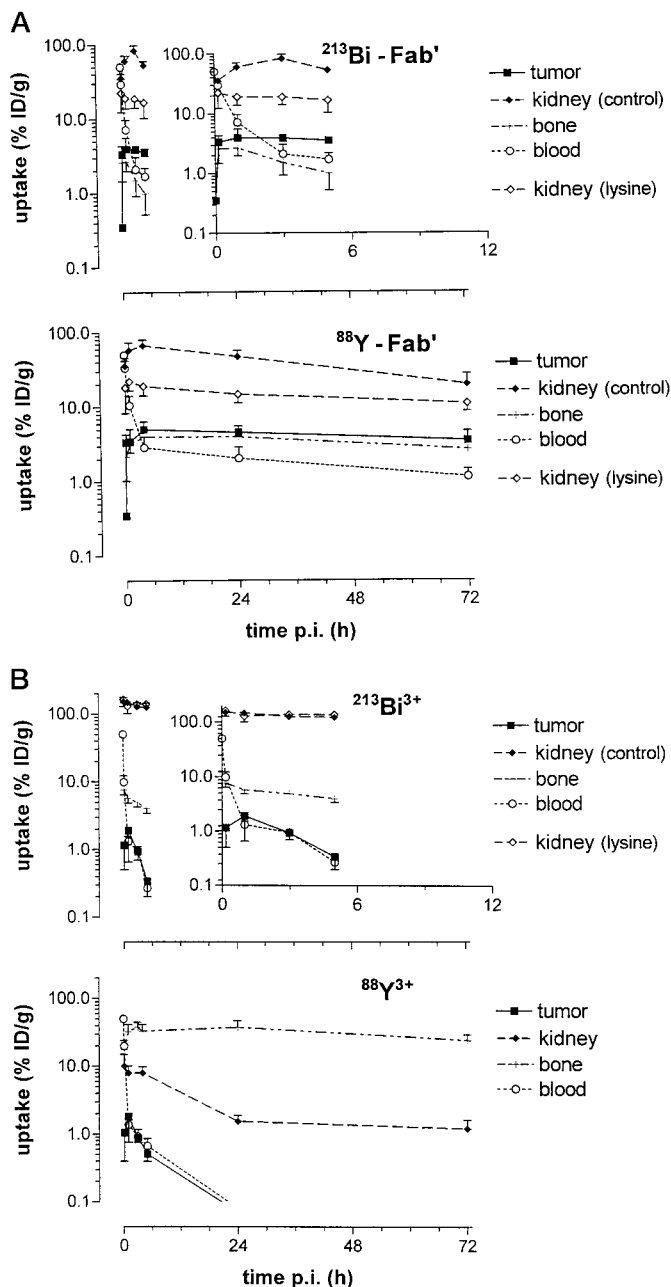


Fig. 1. Biodistribution of ^{213}Bi - and ^{88}Y -labeled CO17-1A Fab' (A) as compared to free $^{213}\text{Bi}^{3+}$ and $^{88}\text{Y}^{3+}$ (B) in the tumor, kidneys, blood, and bone of s.c. GW-39 xenograft-bearing nude mice. The bismuth data are shown with two different time axes (top) to facilitate comparison to the yttrium data.

uptake values of up to $\geq 80\%$ ID/g. As has been published in detail previously (20, 21), application of D-lysine reduced this renal accretion 4–5-fold [Fig. 1a; compare closed diamonds (control kidneys) and open diamonds (kidneys of lysine-treated animals)]. For both ^{213}Bi - and ^{88}Y -labeled CO17-1A Fab', all other organs (e.g., the heart, lungs, liver, spleen, stomach, or intestine) behaved as typical "blood pool organs," with their activity clearances paralleling the blood clearance (data not shown).

In contrast, Fig. 1b shows the biodistribution of the free radiometal ions Bi^{3+} and Y^{3+} . Whereas free bismuth is known to exhibit a very high renal accretion (up to 150% ID/g), which, interestingly, cannot be blocked by lysine (Fig. 1b, top), yttrium ions are well known to be bone-seeking (Fig. 1b, bottom). Fig. 1 clearly demonstrates the good metabolic stability of the Bz-DTPA conjugates used in this study

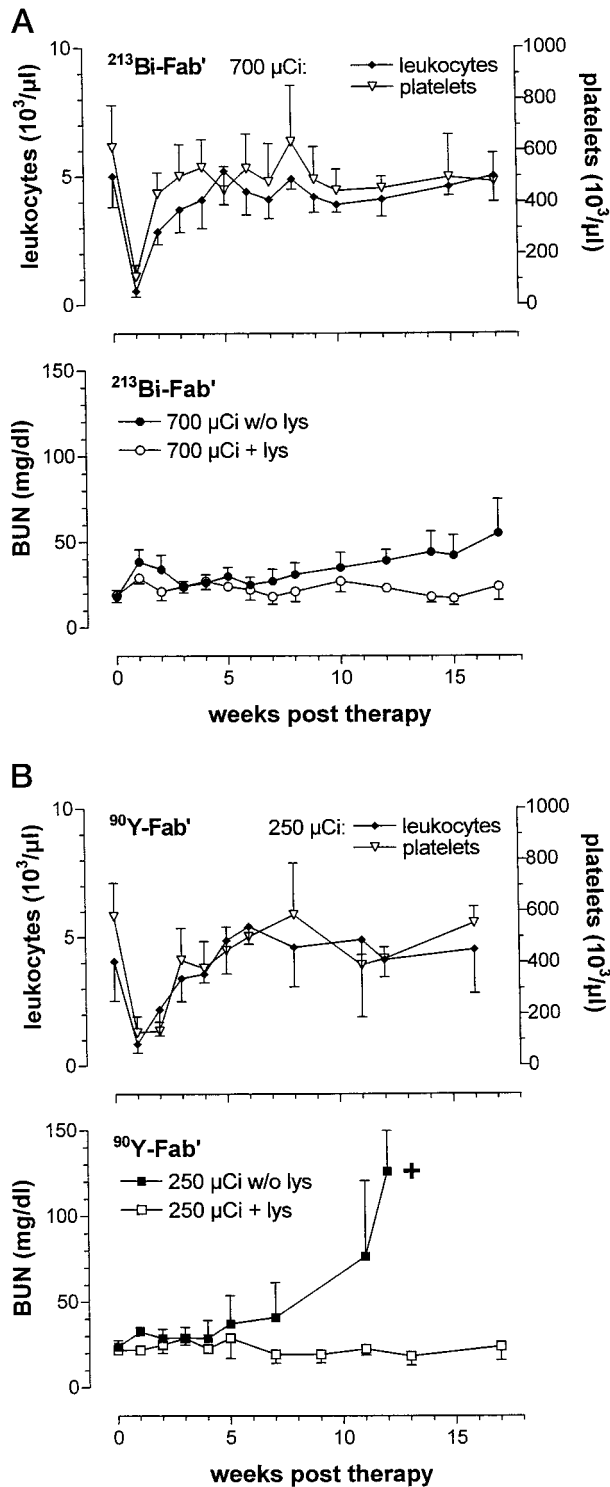


Fig. 2. Myelotoxicity (top) and nephrotoxicity (bottom) of ²¹³Bi-labeled CO17-1A Fab' (A) as compared to ⁹⁰Y-Fab' (B) at their respective MTDs (750 versus 250 µCi) with or without kidney protection by D-lysine administration.

(note the low bone accretion of Y-Fab, with the kidney uptake of bismuth-labeled conjugates not being significantly different from those of their yttrium analogues, as well as the possibility of blocking their renal accretion by lysine, which is in contrast to the persistent renal uptake of free Bi³⁺, despite amino acid administration).

Acute versus Chronic Dose-limiting Toxicity of ²¹³Bi- and ⁹⁰Y-labeled CO17-1A Fab'. MTD-finding trials of ²¹³Bi- and ⁹⁰Y-labeled CO17-1A Fab' were undertaken. For this purpose, varying

amounts of activity were injected, starting at 100 µCi and increasing in 10–20% steps. At each activity level, one group of animals (10–20 per group) received the ²¹³Bi- or ⁹⁰Y-Fab' with no additional support, and a second group was treated with D-lysine. Blood counts (WBCs and platelets) and levels of BUN, creatinine, glutamate oxaloacetate transaminase, and alkaline phosphatase were determined on the day of radioantibody administration and at weekly intervals thereafter. Acute treatment-related death was defined as occurring within 4 weeks post-RIT, whereas later deaths were regarded as chronic toxicity, if these deaths could not be related to tumor growth.

Seven hundred µCi of ²¹³Bi-CO17-1A Fab' and 250 µCi of its ⁹⁰Y-labeled analogue were tolerated by all animals without acute treatment-related lethality, regardless of lysine administration (i.e., the respective MTDs). A 10% increase of these activities resulted in an at least 10% lethality. Fig. 2 shows the blood cell counts (top) and BUN levels (bottom) at these respective maximum tolerated activities for ²¹³Bi- (Fig. 2a) and ⁹⁰Y-Fab' (Fig. 2b), respectively. The nadirs of leukocyte and thrombocyte counts were reached at 1 week after radioantibody administration, and at both respective maximum tolerated activities, the severity of myelotoxicity was not significantly different, regardless of the radionuclide. The recovery from myelotoxicity, however, seems to be faster with the shorter-lived ²¹³Bi than with ⁹⁰Y; with ²¹³Bi-Fab', time to complete recovery was 2–3 weeks posttherapy, but it was 3–4 weeks with ⁹⁰Y-Fab' (compare Fig. 2, a and b, top).

No significant differences with respect to the severity of acute toxicity were observed, whether the animals were given D-lysine or not, and lysine administration alone (without BMT) did not allow for an increase of the MTD, clearly identifying the red marrow as first-line dose-limiting organ. In contrast, profound differences with respect to chronic toxicity were observed between animals given lysine and controls. Fig. 2, bottom, shows that, in non-lysine-treated animals, after a transient (2–3 week) episode of BUN elevation with subsequent normalization, BUN levels began to rise at 6–7 weeks after therapy. As we have observed previously (21), the serum creatinine followed the BUN values but was less sensitive than the latter (data not shown). Surprisingly, the development of chronic renal failure was more dramatic (more steeply rising BUN levels; Fig. 2) in the ⁹⁰Y- than in the ²¹³Bi-treated groups; all animals treated with 250 µCi of ⁹⁰Y-Fab' without lysine protection died within 3 months after therapy, whereas the lethality of animals given 700 µCi of ²¹³Bi-Fab' was only 35% after 6 months.

Lysine-treated groups survived without any signs of renal compromise, and there was no induction of renal insufficiency even six months after treatment (Fig. 2). When kidney protection by lysine was combined with BMT (the latter given at 24 h post-radioantibody administration), the animals survived 400 µCi of ⁹⁰Y- and 1100 µCi of ²¹³Bi-CO17-1A Fab' (i.e., the MTDs with BMT), whereas 10% higher activities again led to an at least 10% lethality. No other signs of second-organ toxicity were observed in any of the treatment groups; e.g., glutamate oxaloacetate transaminase and alkaline phosphatase as indicators of liver function did not show any significant changes, which is in accordance to normal organ doses well below 20 Gy (Table 1).

Comparative Antitumor Efficacy of ²¹³Bi- versus ⁹⁰Y-labeled CO17-1A Fab'. Fig. 3 shows the therapeutic effects of ²¹³Bi- versus ⁹⁰Y-labeled CO17-1A Fab' at their respective MTDs without (Fig. 3a) or with (Fig. 3b) BMT in s.c. GW-39-bearing animals. Both radioconjugates led to a significant ($P < 0.02$) growth retardation as compared to untreated controls or animals treated with the same activities of the Fab' fragment of the irrelevant anti-CD3 antibody OKT3 (the latter not shown). Antitumor effects improved with dose intensification (Fig. 3, a versus b). However, at each MTD (conventional or with BMT) ²¹³Bi-Fab' was therapeutically superior to its ⁹⁰Y

Table 1 Radiation dose estimates of ^{213}Bi - versus ^{90}Y -labeled CO17-1A Fab' in s.c. GW-39 xenograft-bearing nude mice^a

Organ/tissue	^{213}Bi -CO17-1A Fab'				^{90}Y -CO17-1A Fab'		
	Dose (Gy/mCi)		Dose at the MTD		Dose (Gy/mCi)	Dose at the MTD	
	α self-absorption	$\alpha + \beta/\gamma$ with cross-fire	Conventional (Gy/700 μCi)	+ lysine/BMT (Gy/1100 μCi)		β with cross-fire	Conventional (Gy/250 μCi)
Tumor	12.8	13.0	9.1	14.3	54.0	13.5	21.6
Liver	5.6	5.9	4.1		45.4	11.3	
+ lysine	5.7	5.8	4.1	6.4	40.4	10.1	16.2
Spleen	5.7	6.0	4.2		36.7	9.2	
+ lysine	5.7	5.9	4.1	6.5	25.1	6.3	10.0
Kidney	74.2	77.3	54.1		279.2	69.8	
+ lysine	29.3	29.5	20.7	32.5	73.2	18.3	29.0
Lung	6.7	6.9	4.8	7.6	11.6	2.9	4.6
Intestine	2.6	2.9	2.0		37.7	9.4	
+ lysine	2.6	2.8	2.0	3.1	31.2	7.8	12.5
Bone	3.5	3.7	2.6	4.1	27.0	6.8	10.8
Blood	10.5	10.9	7.6	12.0	23.4	5.4	9.4

^a Accounting for cross-organ irradiation, according to the model of Yoriyaz and Stabin (30).

analogue ($P < 0.01$; Fig. 3), whereas no significant differences were observed between both radiolabels with the irrelevant OKT-3 Fab' (data not shown).

Fig. 4a shows the survival of animals bearing GW-39 liver metastases. Groups of 20 animals each were left untreated or given 250 μCi of ^{90}Y -CO17-1A or irrelevant OKT-3 Fab' or 700 μCi of their ^{213}Bi -labeled analogues at 10 days after tumor inoculation, each under kidney protection with D-lysine. The figure shows that untreated animals died within 6–8 weeks of rapidly progressing liver metastases. The survival of animals treated with the irrelevant antibody was prolonged only for 1–3 weeks, regardless of the radiolabel. In contrast, the mean survival of animals treated with ^{90}Y -Fab' was 15 weeks, and 20% of mice treated in this manner survived for >30 weeks. Histology could not demonstrate any viable tumor cells in these long-term survivors, so that these animals were regarded as cured. The cure rate of animals treated with ^{213}Bi -CO17-1A Fab' was, at 95%, highly significantly better ($P < 0.001$) than

with its ^{90}Y analogue. This is in accordance to the macroscopic appearance of animals at 8 weeks after tumor cell inoculation. Fig. 4b shows animals at this very time point, which were left untreated (left), which were given 250 μCi of ^{90}Y -labeled (middle) or 700 μCi of ^{213}Bi -labeled CO17-1A Fab' at a 10-day tumor stage (right). Whereas the liver of untreated animals is grossly enlarged and almost completely replaced by tumor and the livers of animals treated with ^{90}Y -Fab' still clearly contain multiple metastases, no tumor is visible in animals treated with ^{213}Bi -labeled CO17-1A Fab', which is in accordance to their relapse-free long-term survival.

Fig. 5 shows an external scintigraphic scan of two mice bearing multiple GW-39 liver metastases at 1 h after the injection of 700 μCi of ^{213}Bi -labeled CO17-1A Fab' without (left) or with D-lysine administration (right). The scan nicely visualizes the effect of lysine administration on the renal accretion of ^{213}Bi -labeled CO17-1A Fab', and it shows good tumor uptake in multiple metastatic lesions in the liver.

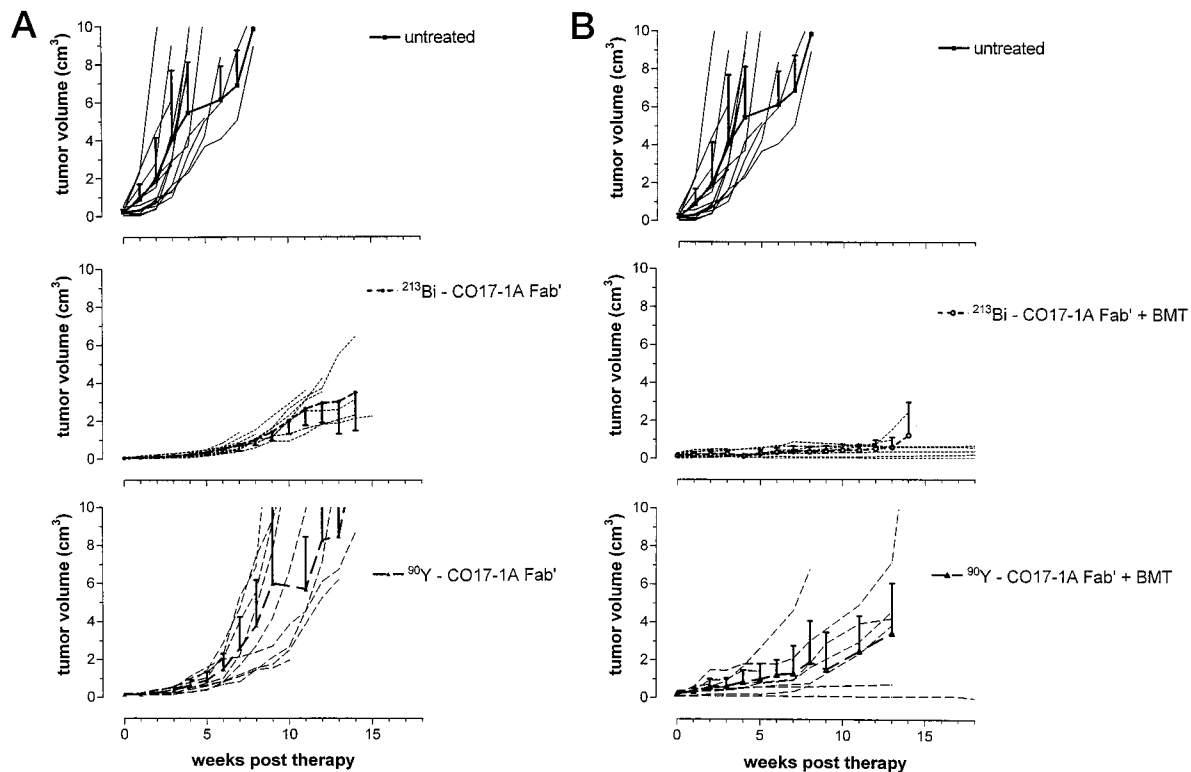


Fig. 3. Therapeutic efficacy of ^{213}Bi - versus ^{90}Y -labeled CO17-1A Fab' as compared to untreated controls at the conventional MTD (700 μCi ^{213}Bi -CO17-1A Fab', 250 μCi ^{90}Y -CO17-1A Fab'; A) and at the MTD with bone marrow support (1100 μCi ^{213}Bi -CO17-1A Fab', 400 μCi ^{90}Y -CO17-1A Fab'; B).

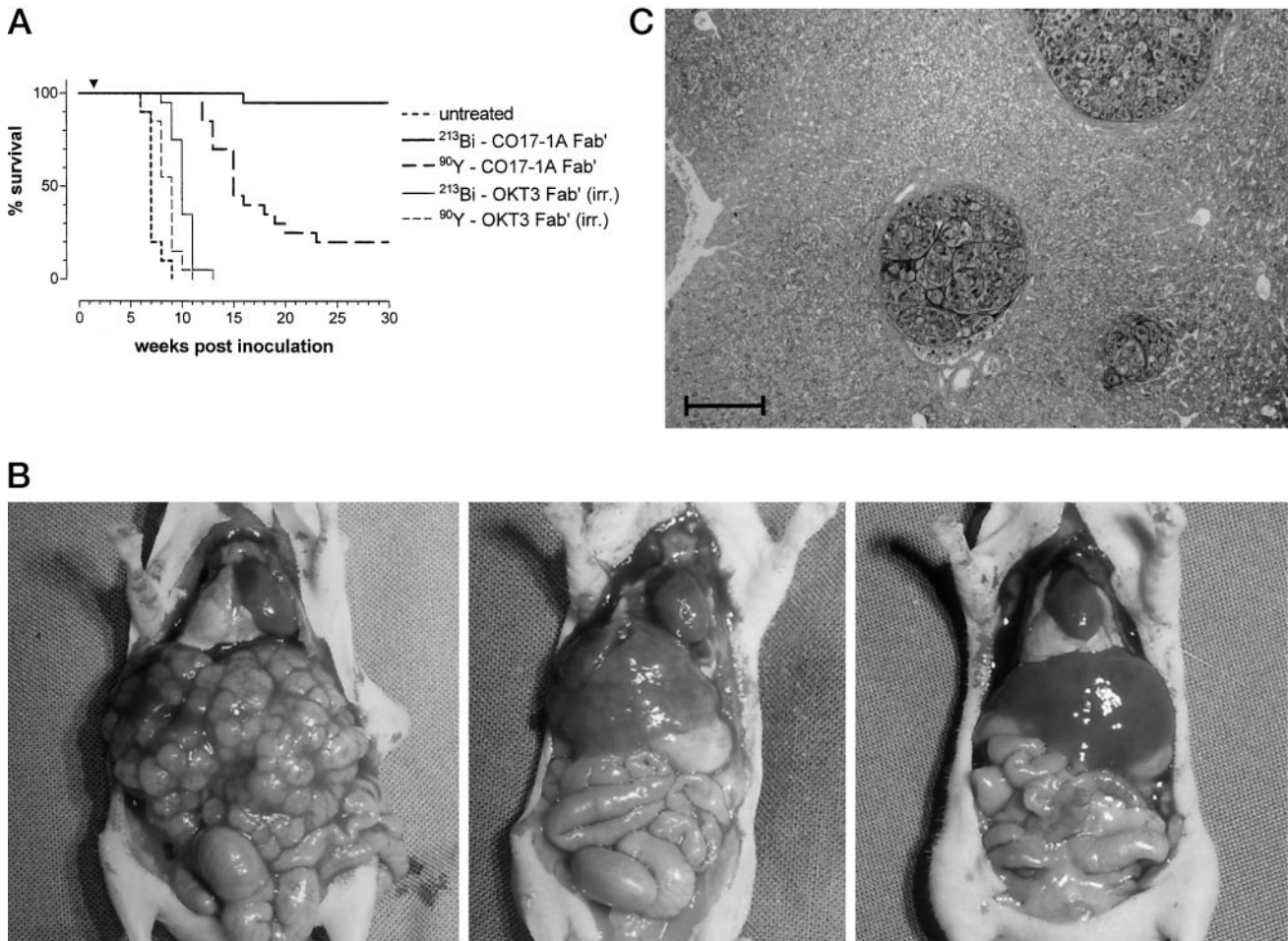


Fig. 4. Therapeutic efficacy of ^{213}Bi - versus ^{90}Y -labeled CO17-1A Fab' as compared to radiolabeled irrelevant Fab' or untreated controls in the GW-39 liver metastasis model. A, survival of animals left untreated or treated at 10 days after tumor inoculation with irrelevant (OKT3) versus specific (17-1A) ^{213}Bi - versus ^{90}Y -labeled Fab' at their respective MTDs. B, macroscopic appearance of animals at 8 weeks after inoculation of tumor cells that were left untreated (left), given 250 μCi of ^{90}Y -labeled (middle), or given 700 μCi of ^{213}Bi -labeled CO17-1A Fab' (right) at a 10-day tumor stage. C, histologically, multiple (as many as over 250) microscopic tumor colonies are present in the livers of these mice, having a size of ~ 250 – 500 μm at this 10-days tumor stage (*i.e.*, the time point of therapy). Scale bar, 100 μm .

Dosimetric Considerations and Correlation of the Observed Biological Effects to the Calculated Radiation Dosimetry. The radiation dosimetry of ^{213}Bi - versus ^{90}Y -labeled CO17-1A Fab' in s.c. GW-39 xenograft-bearing nude mice, based on the biodistribution studies, is summarized in Table 1. Because we have shown previously that, with high-energy β emitters, such as ^{90}Y , cross-organ irradiation may play a major role (32, 38), the model of Yoriyaz and Stabin (30) was used. For the dosimetry of ^{90}Y -CO17-1A Fab', the table accounts for cross-organ radiation, and for ^{213}Bi -Fab', it differentiates into doses resulting merely from the self-absorption of the α particles of ^{213}Po or including the β and γ rays of ^{213}Bi (with potential interorgan cross-fire). As expected for monovalent antibody fragments, the kidneys were the organs with the highest radiation doses. At the conventional MTDs (*i.e.*, 700 μCi of ^{213}Bi - and 250 μCi of ^{90}Y -Fab'), the renal doses were 50–70 Gy without and ~ 20 Gy with lysine protection. This is in accordance with the observed biological effects with chronic radiation nephropathy without amino acid administration, but no significant renal damage was seen with amino acid administration. Interestingly, the blood doses, being representative of the red marrow (39), were also very similar between the two labels (5–8 Gy at the MTD without and 9–12 Gy at the MTD with BMT), regardless of the LET character of the respective emitter. In accordance to the long path length of yttrium-90's β emissions (32, 38), significant cross-fire doses occur from the kidneys to the liver and spleen (compare hepatic

and splenic doses with and without lysine protection), whereas cross-organ doses are negligible with ^{213}Bi .

Fig. 6 shows the relation between calculated tumor doses and the resulting antitumor efficacy (40). As a result of tumor growth retardation being the major observed effect in all treated groups, the correlation between mean tumor doses and the extent of induced growth retardation was analyzed. Because GW-39 is a very rapidly growing cell line with tumor volume doubling times of <1 week (7, 19, 40), the correlation between tumor doses and the mean time needed for the quadruplication of tumor volume (*i.e.*, two doubling times) was analyzed (40). In this graph, individual points represent the tumor volume quadruplication times for the calculated mean tumor doses (as derived from the respective injected activities of ^{213}Bi - versus ^{90}Y -labeled CO17-1A Fab'; Table 1) of different cohorts in separate experiments. With ^{90}Y -Fab', below a tumor dose of ~ 5 Gy, no significant tumor growth delay was noticeable. Above this threshold, tumor growth was retarded in a dose-dependent fashion up to 7-fold at ~ 20 Gy (the highest possible dose at the MTD with BMT). The resulting nonlinear regression curve (regression coefficient: $r = 0.96$) resembles a "shoulder curve," with its shoulder at ~ 5 Gy. In contrast, no threshold dose was seen with ^{213}Bi -CO17-1A Fab'; the time to tumor volume quadruplication was prolonged in an almost linearly increasing manner with increasing tumor dose (regression coefficient: $r = 0.98$). Comparable antitumor efficacy was seen with

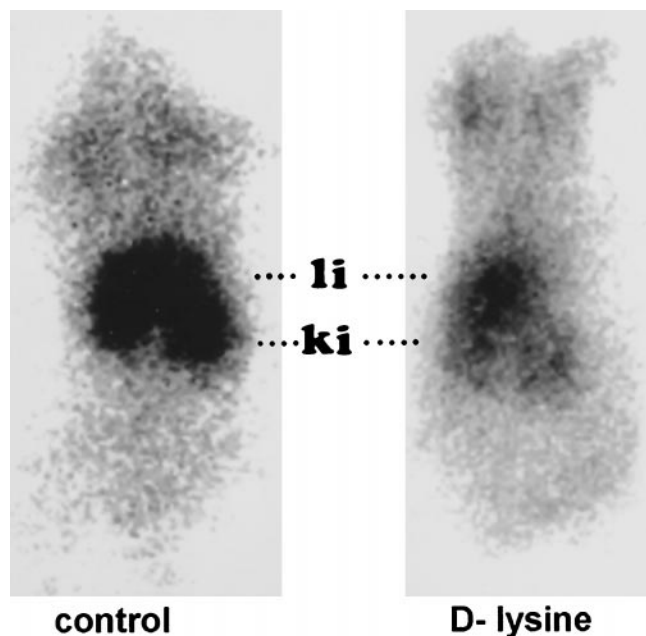


Fig. 5. External scintigraphy (ventral view) of two mice bearing multiple GW-39 liver metastases (3.5 weeks after tumor inoculation) at 1 h after the injection of 700 μ Ci of ^{213}Bi -labeled CO17-1A Fab' without (left) or with D-lysine administration (right). *li*, liver-bearing GW-39 metastases; *ki*, kidney. The camera used was a Picker Prism 2000 large-field-of-view gamma camera, equipped with a high-energy parallel hole-collimator; 100 kcts were acquired in a 440 keV \pm 15% window.

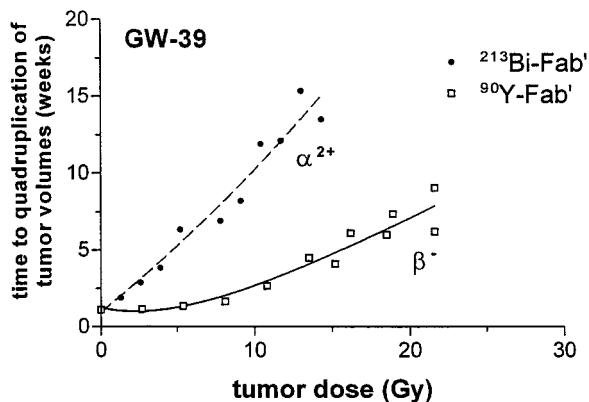


Fig. 6. Dosimetric considerations. Correlation between calculated tumor doses and the resulting antitumor effectiveness (expressed as the time to tumor volume quadruplication relative to untreated controls) for ^{213}Bi - versus ^{90}Y -labeled CO17-1A Fab'. Data points, tumor volume quadruplication times for the calculated mean tumor doses (as derived from the respective injected activities of ^{213}Bi - versus ^{90}Y -labeled CO17-1A Fab'; Table 1) of different cohorts in separate experiments.

^{213}Bi -CO17-1A Fab' at doses that were approximately half to a third as high as those needed with the ^{90}Y label.

DISCUSSION

α particles are monoenergetic, high-energy helium nuclei ($^4\text{He}^{2+}$) with high LET (11). Although there are ~ 100 α -emitting radionuclides, very few possess physical properties that render them potential candidates for medical applications (recently reviewed in Ref. 11). Several authors and studies have postulated or already provided evidence that high-LET radiation emitters may have therapeutic advantages in RIT (reviewed in Ref. 11). The mean LET values of the nuclides tested in this study are 0.2 keV/ μm for the β particles of ^{90}Y , as compared to ~ 100 keV/ μm for the α particles of $^{213}\text{Bi}/\text{Po}$ (for the decay schemes of both

radionuclides, see Table 2; Ref. 11). On the other hand, the mean range in tissue is 3.96 mm for the ^{90}Y β^- as compared to only ~ 0.1 mm for the $^{213}\text{Bi}/\text{Po}$ α^{2+} particles.

^{213}Bi has the advantage that it can be readily obtained from an in-house ^{225}Ac generator, from which it is eluted as $(\text{BiI}_5)^{2-}$ anion (16, 17, 26). Although special bifunctional DTPA derivatives (e.g., cyclohexyl-DTPA) have been designed for bismuth chelation (41), our data using "conventional" bifunctional Bz-DTPA show that this chelator is sufficiently stable, at least with the fast-clearing monovalent antibody fragments used in this study, whereas some earlier data with Bz-DTPA-IgG had shown some loss of bismuth out of chelation over time (42). Our biodistribution data in nude mice show no significant differences in the blood clearance, organ or tumor uptake between ^{213}Bi - or ^{88}Y -labeled Bz-DTPA-derivatized immunoconjugates, indicating sufficient metabolic stability of these Bz-DTPA-Fab' fragments *in vivo*. Incorporation yields were $\geq 90\%$ within a few minutes even at ambient room temperature, requiring < 15 min for the preparation of the final radiolabeled immunoconjugate.

As expected, the tumor uptake was very rapid, which is an important prerequisite for therapy with a short-lived radionuclide such as ^{213}Bi . Also as expected with a monovalent Fab' (20, 21), the kidneys were the organs with the highest physiological uptake. In contrast to the renal accretion of free Bi^{3+} , which could not be prevented by lysine administration (Fig. 1), the renal uptake of both Bi- and Y-labeled Fab' was reduced 5-fold by treatment with cationic amino acids, which is in accordance to our earlier findings (20, 21). The almost identical biodistribution of both Bi- and Y-labeled conjugates confirms, together with the low bone accretion of the Y-conjugates, the fact that bifunctional DTPA derivatives are sufficiently stable for both radionuclides *in vivo*, although further improved metabolic stability may be gained by using the more rigid, bifunctional cyclohexyl-DTPA backbone mentioned above (41, 43).

As we reported previously for ^{90}Y -labeled Fab fragments (21, 38), with respect to acute radiation toxicity, the bone marrow is the first-line dose-limiting organ with ^{213}Bi -labeled Fab' fragments as well. The nadirs of WBC and platelet counts were similar between both α emitter- and β emitter-labeled conjugates, but interestingly, the peripheral blood counts recovered faster from the bone marrow injury by the high-LET but shorter-lived ^{213}Bi than by the low-LET but longer-lived ^{90}Y (Fig. 2). This observation is in accordance with earlier observations of the dependence of bone marrow recovery upon the effective half-life of the radioconjugate in the blood or bone marrow (19, 32). Most surprising, however, is the observation that the maximum tolerated blood doses, which are generally accepted as representative of the red marrow doses (the latter being difficult to

Table 2 Physical characteristics of ^{213}Bi and its progeny as compared to ^{90}Y

Radionuclide	Half-life	Emission (%) ^a	Emissions	Particle energy ^b
^{213}Bi	45.6 min	98	β^-	1.4 MeV
		17	γ	440 keV
		2	α	5.9 MeV
	4.2 μs	98	α	8.4 MeV
^{209}Pb	3.25 h	100	β^-	0.6 MeV
^{209}Bi	Stable			

^{90}Y	64.1 h	100	β^-	2.3 MeV
^{90}Zr	Stable			

^a Percentage emitted per decay of the respective parent radionuclide.

^b Maximum β^- and approximate α energies are listed.

assess directly; Ref. 39), were almost identical for both low- and high-LET radiation (Table 1). This is in sharp contrast to the general assumption of a RBE factor of 10–20 for α particles (44–46). This assumption relies on earlier *in vitro* data. However, this factor has never been reproducible *in vivo*, and more recent studies have shown that the RBE *in vivo* is dependent upon the α particle energy and the LET (47, 48). In a mouse testes spermatogenesis model, Howell *et al.* (47, 48) demonstrated RBE values between 3 and 9 (the higher the α particle energy, the lower the RBE). Even more important, Charlton *et al.* (49) modeled the hemopoietic stem cell survival following irradiation by α particles of various energies, using Monte Carlo methodology to calculate passages of α particles, originating in three geometries, through the nuclei of the stem cells. Survival predictions were made from probability mapping of surviving each passage as a function of LET. These authors predicted, for α particles of various energies, RBE values that lie between 1.5 and 2.1 in the human red marrow, depending upon their energy (again, the higher the energy, the lower the RBE), with a predicted RBE of ~ 1.5 for the 8.4-MeV α particles of $^{213}\text{Bi}/^{213}\text{Po}$ (49). When the maximum tolerated blood doses of ^{213}Bi -Fab' are compared to those of ^{90}Y -Fab' (cf. Table 1), the MTD with the α emitter appears to be even slightly higher than the one with the low-LET β^- emitter. Thus, most surprisingly, our data suggest an *in vivo* RBE value with respect to bone marrow toxicity of close to one as compared to low-LET β^- radiation. Given the relatively long (0.1 mm) path length of the high (8.4-MeV) energy α particles of $^{213}\text{Bi}/^{213}\text{Po}$, it appears unlikely that heterogeneity of the microdistribution may cause these effects, but future studies must address this point in more detail. However, recent human data with the ^{213}Bi -labeled anti-CD33 antibody HuM195 also seem to confirm an *in vivo* RBE value with respect to bone marrow toxicity of close to 1, as compared to low-LET β or γ radiation (50).⁵

Radiation-induced renal toxicity is a major concern in the therapeutic application of antibody fragments or peptides radiolabeled with metals. We have shown previously (21, 51) that, for ^{90}Y -labeled conjugates, two distinct pathological features must be distinguished in this context: kidney doses of more than ~ 100 Gy result, within 1–2 weeks, in an acute renal failure which is histologically characterized by an acute tubular necrosis; this form of acute radiation nephritis is lethal within hours or a few days of its onset. In contrast, at doses between ~ 60 and 100 Gy, very few or no symptoms are found in the first weeks after the irradiation, but progressive chronic renal failure develops within months; histologically, this pathophysiological entity is characterized by a progressive glomerular sclerosis, tubular atrophy, arteriolar intimal fibrosis, and severe interstitial scarring (21, 51). This more chronic form of radiation nephropathy corresponds to the clinically well known syndrome of "chronic radiation nephritis," which is characterized by hypertension (moderate to malignant), edema, proteinuria, anemia, and uremia (21, 51). Interestingly, in contrast to earlier studies (21), non-lysine-protected animals showed a short episode of transient slight but significant BUN elevation, whereas BUN levels remained low in lysine-treated animals. However, after ~ 4 –6 weeks, BUN levels steadily begin to rise in animals treated at the MTD without lysine protection (Fig. 2). The development of terminal renal insufficiency was more rapid and more dramatic with ^{90}Y than with ^{213}Bi , which would be in accordance with the radiation dosimetry (70 versus 54 Gy to the kidneys), but again, this result is highly surprising, because one would expect a much higher biological efficacy of the high-LET α emitter. Obviously, α particle RBE values are lower than originally expected in kidneys as

well, similar to our observations in the bone marrow (see above). Most importantly however, none of the lysine-protected animals developed signs of radiation nephropathy, and histology also failed to show significant alterations, which holds true for animals given a dose-intensified treatment regimen with BMT as well.

At equitoxic dosing (either at dose levels below the conventional MTD, at the conventional MTD, or at the MTD with BMT), RIT with ^{213}Bi -Fab' was therapeutically superior to its conventional β -emitting ^{90}Y analogue. The same holds true for the liver metastatic model, in which ^{213}Bi -Fab' resulted in a $>90\%$ cure rate, in contrast to only 20% with ^{90}Y . Although, due to its long path length, ^{90}Y may not be the ideal radionuclide for treating micrometastases, cure rates with the shorter-range ^{131}I -Fab' were very comparable to those with ^{90}Y -Fab', as presented here (52),^{4,6} supporting our view that the superiority of ^{213}Bi is not just due to the shorter path length of its α particles. Thus, the high-LET α emitter clearly appears therapeutically superior to the conventional low-LET radiation emitters. This is in accordance to the earlier findings of Bloomer *et al.* (18), who compared the therapeutic efficacy of α -emitting (^{211}At) and β -emitting (^{32}P , ^{90}Y , and ^{165}Dy) radiocolloids for the treatment of experimental malignant ascites and demonstrated an unequivocal advantage for the high-LET α emitter.

We have shown earlier that plotting tumor volume multiplication times against tumor doses (Fig. 6) yields a diagram resembling a sort of inverted cell survival curves (7, 19, 40) known from external beam radiation of cells in cell culture (45, 46). This is not surprising, because the tumor volume is a function of the total number of cells, and the change in tumor volume is a function of the number of viable cells that are able to proliferate. Below tumor doses of ~ 5 –10 Gy, the effects on tumor growth delay were minimal. In contrast, the tumor volume multiplication curve under ^{213}Bi -treatment lacks a pronounced shoulder and displays an almost linearly increasing efficacy with increasing dose. Interestingly, comparable antitumor efficacy with ^{213}Bi results at approximately half to one-third of the doses needed with ^{90}Y . This is very similar to the improved antitumor efficacy which we have demonstrated earlier for Auger/conversion electron emitters internalized into the cytoplasm of the tumor cells (7).

In summary, the data of this study show that RIT with α emitters may be therapeutically more effective than RIT with conventional β emitters. Surprisingly, the red marrow and the kidney seem to tolerate similar radiation doses of the high-LET α as compared to the low-LET β emitters, whereas the RBE in the tumor is 2–3-fold higher, providing a clear therapeutic advantage in favor of the high-LET α emitter. Furthermore, radiation nephrotoxicity of the antibody fragments can be overcome by basic amino acid administration. Due to its short physical $t_{1/2}$, ^{213}Bi appears to be especially suitable for use in conjunction with fast-clearing fragments; its 440-keV γ emission also can be used for quantitation by external scintigraphy.

ACKNOWLEDGMENTS

We thank Dr. O. Proske (Glaxo Wellcome, Inc., Hamburg, Germany), for providing us with the CO17-1A MAb. The expert advice of Prof. Dr. M. Oellerich (Department of Clinical Chemistry, Georg-August-University of Göttingen, Göttingen, Germany) with respect to blood count determinations and blood chemistry is gratefully acknowledged. Furthermore, we thank Drs. K. Nebendahl and O. Schunck (Animal Care Facility, Georg-August-University of Göttingen) for their valuable advice with respect to animal care.

REFERENCES

1. Goldenberg, D. M. (ed.). *Cancer Therapy with Radiolabeled Antibodies*. Boca Raton, FL: CRC Press, 1995.
- 6 T. M. Behr, A. L. Salib, D. M. Goldenberg, and W. Becker, unpublished results.

⁵ J. G. Jurcic, Å. Ballangrud, D. A. Scheinberg, and G. Sgouros, personal communication.

2. Kaminski, M. S., Zasadny, K. R., Francis, I. R., Milik, A. W., Ross, C. W., Moon, S. D., Crawford, S. M., Burgess, J. M., Petry, N. A., Butchko, G. M., and Wahl, R. L. Radioimmunotherapy of B-cell lymphoma with [^{131}I]anti-B1 (anti-CD20) antibody. *N. Engl. J. Med.*, 329: 459–465, 1993.
3. Press, O. W., Eary, J. F., Appelbaum, F. R., Martin, P. J., Nelp, W. B., Glenn, S., Fisher, D. R., Porter, B., Matthews, D. C., Gooley, T., and Bernstein, I. D. Phase II trial of ^{131}I -B1 (anti-CD20) antibody therapy with autologous stem cell transplantation for relapsed B cell lymphoma. *Lancet*, 346: 336–340, 1995.
4. Behr, T. M., Sharkey, R. M., Juweid, M. E., Dunn, R. M., Vagg, R. C., Ying, Z., Zhang, C. H., Swayne, L. C., Vardi, Y., Siegel, J. A., and Goldenberg, D. M. Phase I/II clinical radioimmunotherapy with an ^{131}I -labeled anti-CEA murine IgG monoclonal antibody. *J. Nucl. Med.*, 38: 858–870, 1997.
5. Behr, T. M., Sharkey, R. M., Juweid, M. E., Dunn, R. M., Siegel, J. A., and Goldenberg, D. M. Factors influencing the pharmacokinetics, dosimetry, and diagnostic accuracy of radioimmuno-detection and radioimmunotherapy of CEA-expressing tumors. *Cancer Res.*, 56: 1805–1816, 1996.
6. Woo, D. V., Li, D., Mattis, J. A., and Steplewski, Z. Selective chromosomal damage and cytotoxicity of ^{125}I -labeled monoclonal antibody 17-1a in human cancer cells. *Cancer Res.*, 49: 2952–2958, 1989.
7. Behr, T. M., Sgouros, G., Vougioukas, V., Memtsoudis, S., Gratz, S., Schmidberger, H., Goldenberg, D. M., and Becker, W. Therapeutic efficacy and dose-limiting toxicity of Auger-electron versus β emitters in radioimmunotherapy with internalizing antibodies: Evaluation of ^{125}I - versus ^{131}I -labeled CO17-1A in a human colorectal cancer model. *Int. J. Cancer*, 76: 738–748, 1998.
8. Meredith, R. F., Khazaeli, M. B., Plott, W. E., Spencer, S. A., Wheeler, R. H., Brady, L. W., Woo, D. V., and LoBuglio, A. F. Initial clinical evaluation of iodine-125-labeled chimeric 17-1A for metastatic colon cancer. *J. Nucl. Med.*, 36: 2229–2233, 1995.
9. Welt, S., Scott, A. M., Divgi, C. R., Kemeny, N. E., Finn, R. D., Daghighian, F., St. Germain, J., Richards, E. C., Larson, S. M., and Old, L. J. Phase I/II study of iodine-125-labeled monoclonal antibody A33 in patients with advanced colon cancer. *J. Clin. Oncol.*, 14: 1787–1797, 1996.
10. Zalutsky, M. R., Garg, P. K., Friedman, H. S., and Bigner, D. D. Labeling monoclonal antibodies and F(ab')₂ fragments with the α -particle-emitting nuclide astatine-211: preservation of its immunoreactivity and *in vivo* localizing capacity. *Proc. Natl. Acad. Sci. USA*, 86: 7149–7153, 1989.
11. McDevitt, M. R., Sgouros, G., Finn, R. D., Humm, J. L., Jurcic, J. G., Larson, S. M., and Scheinberg, D. A. Radioimmunotherapy with α -emitting nuclides. *Eur. J. Nucl. Med.*, 25: 1341–1351, 1998.
12. Zalutsky, M. R., and Narula, A. S. Astatination of proteins using an *N*-succinimidyl tri-*n*-butylstannyl benzoate intermediate. *Int. J. Radiat. Appl. Instrum. A*, 39: 227–232, 1988.
13. Vaidyanathan, G., Affleck, D., and Zalutsky, M. R. Monoclonal antibody F(ab')₂ fragment labeled with *N*-succinimidyl-2,4-dimethoxy-3-halobenzoates: *in vivo* comparison of iodinated and astatinated fragments. *Nucl. Med. Biol.*, 21: 105–110, 1994.
14. Macklis, R. M., Kinsey, B. M., Kassis, A. L., Ferrara, J. L. M., Atcher, R. W., Hines, J. J., Coleman, C. N., Adelstein, S. J., and Burackhoff, S. J. Radioimmunotherapy with α -particle-emitting immunoconjugates. *Science (Washington DC)*, 240: 1024–1026, 1988.
15. Kurtzman, S. H., Russo, A., Mitchell, J. B., DeGraff, W., Sindelar, W. F., Brechbiel, M. W., Gansow, O. A., Friedman, A. M., Hines, J. J., Gamson, J., and Atcher, R. W. Bismuth-212 linked to an antipancratic carcinoma antibody: model for α -particle-emitter radioimmunotherapy. *J. Natl. Cancer Inst. (Bethesda)*, 80: 449–452, 1988.
16. Geerlings, M. W., Kaspersen, F. M., Apostolidis, C., and Van der Hout, R. The feasibility of ^{225}Ac as a source of α -particles in radioimmunotherapy. *Nucl. Med. Commun.*, 14: 121–125, 1993.
17. Kaspersen, F. M., Bos, E., Doornmalen, A. V., Geerlings, M. W., Apostolidis, C., and Molinet, R. Cytotoxicity of ^{213}Bi - and ^{225}Ac -immunoconjugates. *Nucl. Med. Commun.*, 16: 468–476, 1995.
18. Bloomer, W. D., McLaughlin, W. H., Lambrecht, R. M., Atcher, R. W., Mirzadeh, S., Madara, J. L., Milius, R. A., Zalutsky, M. R., Adelstein, S. J., and Wolf, A. P. ^{211}At radiocolloid therapy: further observations and comparison with radiocolloids of ^{32}P , ^{165}Dy , and ^{90}Y . *Int. J. Radiat. Oncol. Biol. Phys.*, 10: 341–348, 1984.
19. Behr, T. M., Memtsoudis, S., Sharkey, R. M., Blumenthal, R. D., Dunn, R. M., Gratz, S., Wieland, E., Nebendahl, K., Schmidberger, H., Goldenberg, D. M., and Becker, W. Experimental studies on the role of antibody fragments in cancer radioimmunotherapy: influence of radiation dose and dose rate on toxicity and antitumor efficacy. *Int. J. Cancer*, 77: 787–795, 1998.
20. Behr, T. M., Sharkey, R. M., Juweid, M. E., Blumenthal, R. D., Dunn, R. M., Bair, H. J., Griffiths, G. L., Wolf, F. G., Becker, W. S., and Goldenberg, D. M. Reduction of the renal uptake of radiolabeled monoclonal antibody fragments by cationic amino acids and their derivatives. *Cancer Res.*, 55: 3825–3834, 1995.
21. Behr, T. M., Sharkey, R. M., Sgouros, G., Blumenthal, R. D., Dunn, R. M., Kolbert, K., Griffiths, G. L., Siegel, J. A., Becker, W. S., and Goldenberg, D. M. Overcoming the nephrotoxicity of radiometal-labeled immunoconjugates: improved cancer therapy administered to a nude mouse model in relation to the internal radiation dosimetry. *Cancer (Phila.)*, 80: 2591–2610, 1997.
22. Herlyn, M., Steplewski, Z., Herlyn, D., and Koprowski, H. Colorectal carcinoma-specific antigen: detection by means of monoclonal antibodies. *Proc. Natl. Acad. Sci. USA*, 76: 1438–1442, 1979.
23. Koprowski, H., Steplewski, Z., Mitchell, K., Herlyn, M., Herlyn, D., and Fuhrer, J. P. Colorectal carcinoma antigens detected by hybridoma antibodies. *Somat. Cell Genet.*, 5: 957–972, 1979.
24. Göttlinger, H. G., Funke, I., Johnson, J. P., Gokel, J. M., and Riethmüller, G. The epithelial surface antigen 17-1A, a target for antibody-mediated tumour therapy: its biochemical nature, tissue distribution and recognition by different monoclonal antibodies. *Int. J. Cancer*, 38: 47–53, 1986.
25. Brechbiel, M. W., Gansow, O. A., Achter, R. W., Schlom, J., Esteban, J. M., Simpson, D. E., and Colcher, D. Synthesis of 1-(*p*-isothiocyanobenzyl) derivatives of DTPA and EDTA: antibody labeling and tumor imaging studies. *Inorg. Chem.*, 25: 2772–2781, 1986.
26. Spivakov, B. Y., Stoyanov, E. S., Gribov, L. A., and Zolotov, Y. A. Raman laser spectroscopic studies of bismuth(III) halide complexes in aqueous solutions. *J. Inorg. Nucl. Chem.*, 41: 453–455, 1979.
27. Boll, R. A., Mirzadeh, S., Kennel, S. J., DePaoli, D. W., and Webb, O. F. ^{213}Bi for α -particle-mediated radioimmunotherapy. *J. Lab. Comput. Radiopharm.*, XL: 341, 1997.
28. Van Geel, J. N. C., Fuger, J., and Koch, L. Verfahren zur Erzeugung von Actinium-225 und Wismuth-213, European Patent No. 0 443 479 B1, 1994.
29. Goldenberg, D. M., Witte, S., and Elster, K. GW-39: a new human tumor serially transplantable in the golden hamster. *Transplantation (Baltimore)*, 4: 760–764, 1966.
30. Yoriyaz, H., and Stabin, M. Electron and photon transport in a model of a 30g mouse. *J. Nucl. Med.*, 38: 228P, 1997.
31. Briesmeister, J. MCNP: A General Monte Carlo n-Particle Transport Code. MCNP User's Manual. Los Alamos, NM: Los Alamos National Laboratory, 1993.
32. Behr, T. M., Sgouros, G., Stabin, M. G., Béhé, M., Angerstein, C., Blumenthal, R. D., Apostolidis, C., Molinet, R., Sharkey, R. M., Koch, L., Goldenberg, D. M., and Becker, W. Studies on the red marrow dosimetry in radioimmunotherapy: an experimental investigation of factors influencing the radiation-induced myelotoxicity in therapy with β -, Auger/conversion electron-, or α -emitters. *Clin. Cancer Res.*, in press, 1999.
33. Blumenthal, R. D., Sharkey, R. M., Forman, D., Wong, G., Hess, J., and Goldenberg, D. M. Improved experimental cancer therapy by radioantibody dose intensification as a result of syngeneic bone marrow transplantation. *Exp. Hematol.*, 23: 1088–1097, 1995.
34. Sharkey, R. M., Blumenthal, R. D., Behr, T. M., Wong, G. Y., Haywood, L., Forman, D., Griffiths, G. L., and Goldenberg, D. M. Selection of radioimmunoconjugates for the therapy of well-established or micrometastatic colon carcinoma. *Int. J. Cancer*, 72: 477–485, 1997.
35. Wilcoxon, F. Individual comparisons by ranking methods. *Biometrics*, 1: 80–83, 1945.
36. Sprent, P. Applied Nonparametric Statistical Methods, Ed. 2. London: Chapman & Hall, 1993.
37. Bowalekar, S. K. Statistics in medical research: IV. Sampling distribution, statistical testing of hypothesis and Student's *t*-test. *J. Postgrad. Med.*, 40: 46–51, 1994.
38. Behr, T. M., Sgouros, G., Sharkey, R. M., Dunn, R. M., Blumenthal, R. D., Kolbert, K., Siegel, J. A., and Goldenberg, D. M. Y-90-dosimetry in nude mice requires accounting for cross-organ radiation: evaluation of three dosimetry models in relation to observed biological effects. *J. Nucl. Med.*, 37: 102P, 1996.
39. Sgouros, G. Bone marrow dosimetry for radioimmunotherapy: theoretical considerations. *J. Nucl. Med.*, 34: 689–694, 1993.
40. Behr, T. M., Wulst, E., Radetzky, S., Blumenthal, R. D., Dunn, R. M., Gratz, S., Rave-Fränk, M., Schmidberger, H., Raue, F., and Becker, W. Improved treatment of medullary thyroid cancer in a nude mouse model by combined radioimmunotherapy: doxorubicin potentiates the therapeutic efficacy of radiolabeled antibodies in a radioresistant tumor type. *Cancer Res.*, 57: 5309–5319, 1997.
41. Wu, C., Kobayashi, H., Sun, B., Yoo, T. M., Paik, C. H., Gansow, O. A., Carrasquillo, J. A., Pastan, I., and Brechbiel, M. W. Stereochemical influence on the stability of radio-metal complexes *in vivo*. Synthesis and evaluation of the four stereoisomers of 2-(*p*-nitrobenzyl)-*trans*-CyDTPA. *Bioorg. Med. Chem.*, 5: 1925–1934, 1997.
42. Ruegg, C. L., Anderson-Berg, W. T., Brechbiel, M. W., Mirzadeh, S., Gansow, O. A., and Strand, M. Improved *in vivo* stability and tumor targeting of bismuth-labeled antibody. *Cancer Res.*, 50: 4221–4226, 1990.
43. Hartmann, F., Horak, E. M., Garmestani, K., Wu, C., Brechbiel, M. W., Kozak, R. W., Tso, J., Kostein, S. A., Gansow, O. A., and Nelson, D. L. Radioimmunotherapy of nude mice bearing a human interleukin 2 receptor α -expressing lymphoma utilizing the α -emitting radionuclide-conjugated monoclonal antibody ^{212}Bi -anti-Tac. *Cancer Res.*, 54: 4362–4370, 1994.
44. Hendry, J. H., and Lord, B. I. (eds.). Radiation Toxicology: Bone Marrow and Leukaemia. London: Taylor & Francis, 1995.
45. Hall, E. J. Radiobiology for the Radiologist. Philadelphia: J. B. Lippincott, 1994.
46. Walden Jr, T. L., and Farzaneh, N. K. Biochemistry of Ionizing Radiation. New York: Raven Press, 1990.
47. Howell, R. W., Azure, M. T., Narra, V. R., and Rao, D. V. Relative biological effectiveness of α -emitters *in vivo* at low doses. *Radiat. Res.*, 137: 352–360, 1994.
48. Howell, R. W., Goddu, S. M., Narra, V. R., Fisher, D. R., Schenter, R. E., and Rao, D. V. Radiotoxicity of gadolinium-148 and radium-223 in mouse testes: relative biological effectiveness of α -particle emitters *in vivo*. *Radiat. Res.*, 147: 342–348, 1997.
49. Charlton, D. E., Utteridge, T. D., and Allen, B. J. Theoretical treatment of human haemopoietic stem cell survival following irradiation by α particles. *Int. J. Radiat. Biol.*, 74: 111–118, 1998.
50. Jurcic, J. G., McDevitt, M. R., Sgouros, G., Ballangrud, Å., Finn, R. D., Geerlings, M. W., Humm, J. L., Molinet, R., Apostolidis, C., Larson, S. M., and Scheinberg, D. A. Targeted α -particle therapy for myeloid leukemias: a Phase I trial of bismuth-213-HuM195 (anti-CD33). *Blood*, 90 (Suppl.): 504a, 1997.
51. Behr, T. M., Goldenberg, D. M., and Becker, W. Reducing the renal uptake of radiolabeled antibody fragments and peptides for diagnosis and therapy: present status, future prospects and limitations. *Eur. J. Nucl. Med.*, 25: 201–212, 1998.
52. Behr, T. M., Salib, A., Gratz, S., Béhé, M., Yücekent, S., Blumenthal, R. D., Sharkey, R. M., Goldenberg, D. M., and Becker, W. Radioimmunotherapy of colorectal cancer in small volume disease: evaluation of radioimmunotherapy versus standard chemotherapy in a nude mouse model of human colon cancer metastatic to the liver. *Eur. J. Nucl. Med.*, 25: 894, 1998.